SUSTAINABLE SYNTHESIS OF PAR-MODIFIED CHITOSAN FOR SELECTIVE LEAD(II) SEPARATION FROM COPPER(II) IN WATER

Piotr Kotlarczyk[1,a], Łukasz Wujcicki[2,b], Tomasz Mańdok[2,c], Jakub Adamek[3,d], Joanna Kluczka[2,e,*]

[1] – Silesian University of Technology, Faculty of Chemistry, ks. M. Strzody 9 Str., 44-100 Gliwice, Poland
[a] – ORCID: 0009-0003-9338-9560
[2] – Silesian University of Technology, Faculty of Chemistry, Department of Inorganic, Analytical and Electrochemistry, B. Krzywoustego 6 Str., 44-100 Gliwice, Poland
[b] – ORCID: 0009-0008-2475-150X, [c] – ORCID: 0009-0004-6021-1843,
[e] – ORCID: 0000-0002-4937-7832
[3] – Silesian University of Technology, Faculty of Chemistry, Department of Organic, Bioorganic Chemistry and Biotechnology, B. Krzywoustego 8 Str., 44-100 Gliwice, Poland
[d] – ORCID: 0000-0002-2960-6247
**corresponding author: joanna.kluczka@polsl.pl*

Abstract

Elevated concentrations of lead and copper in the natural environment, primarily due to polymetallic ore processing, underscore the urgent need for advanced remediation strategies. The chemical similarity between these metals complicates their selective separation during water treatment. Chitosan-based adsorbents, which are both biodegradable and environmentally benign, offer a promising approach. In this study, a derivative of the 4-(2-pyridylazo)resorcinol (PAR) was synthesised and used in a sustainable mechanochemical process to modify chitosan. The modified material was characterised by ^{13}C NMR and FTIR spectroscopy, and its adsorption properties were evaluated using ICP-AES. The PAR-derivative-modified chitosan exhibited high adsorption efficiency for lead ions (95.4%) and lower efficiency for copper ions (38.3%). These findings indicate that chitosan-based materials can be effective for heavy metal adsorption removal and possess significant potential for the selective separation of Pb(II) from Cu(II).

Keywords: *sorption, chitosan, lead, copper, 4-(2-pyridylazo)resorcinol, separation process*

Received: 01.04.2026
Accepted: 23.07.2026

1. Introduction

Heavy metals are a significant concern among environmental pollutants due to their toxicity [1, 2]. Within this group, lead and copper are currently of particular interest.

Lead exposure in humans can result in cognitive impairment and damage to multiple organs, including the kidneys, reproductive system, and nervous system [3]. In contrast, copper is essential at low concentrations but becomes toxic at higher levels (the LD50 of copper(II) sulfate administered orally to rats is 30 mg/kg) [4]. Elevated levels of copper are associated with cardiovascular diseases: coronary heart disease, chronic heart failure, coronary artery disease, rheumatic heart disease, atherosclerosis, and myocardial infarction [5].

Lead and copper are among the most prevalent heavy metals found in contaminated water. These metals can enter drinking water through the corrosion of pipes composed of lead, copper, or their alloys, such as brass [6]. In response, the US Environmental Protection Agency introduced the Copper and Lead Rule in 1991, which established permissible levels of copper and lead in drinking water and outlined appropriate consumer-level monitoring rather than solely at distribution points. Implementation of this regulation has reduced lead and copper concentrations in water and prompted the replacement of non-compliant installations. These measures have contributed to the prevention of birth defects in newborns and a reduction in heart disorders and brain damage in children [7–9].

A significant challenge in water treatment is the frequent coexistence of lead and copper in aqueous systems, primarily due to shared anthropogenic sources, such as mining, metallurgy, and fossil fuel production, as well as corrosion of water distribution infrastructure [10]. Their similar chemical behaviour, especially in ionic form and coordination properties, complicates selective separation. Nevertheless, selective removal is necessary to reduce overall water toxicity because these metals have distinct toxicological profiles that may warrant individual removal or recovery.

Numerous techniques have been developed to remove heavy metals from aqueous solutions, including precipitation, filtration and ultrafiltration, ion exchange, reverse osmosis, coagulation, flocculation, electrodialysis, flotation, and adsorption [11]. Many of these methods require additional chemicals and can be costly. Among these, adsorption is notable for its ongoing development and its ability to address the limitations of other methods [12]. The modifiability of adsorbents enables more effective contaminant removal. A key advantage of adsorption is its selectivity, which enables targeted removal of specific pollutants and the regeneration of used adsorbents. The reversible nature of adsorption and the possibility of desorption also reduce waste generation, making it an environmentally beneficial solution [13].

Multiple strategies have been explored to optimise the adsorption process, with chitosan identified as a particularly promising material. Chitosan is a natural polymer derived from the deacetylation of chitin, which is abundant in renewable materials such as crustacean shell waste [14]. It is biodegradable, biocompatible, and non-toxic, making it suitable for environmentally sustainable applications [15]. The presence of amino and hydroxyl functional groups in its structure facilitates effective interaction with metal ions. However, native chitosan shows limited selectivity in complex systems containing multiple metal ions, limiting its use for selective separation. To address these limitations, modification strategies have been developed, including the introduction of organic ligands or substances such as iron or aluminum oxides [16], as well as polymer cross-linking with various agents [17].

Several studies have addressed the adsorption-based removal of lead and copper ions from aqueous solutions. Rangel-Méndez *et al.* [18] evaluated native chitosan for the adsorption of Pb(II) and Cu(II) ions, demonstrating its affinity for these metals. However, the study noted that chitosan's limited selectivity complicates the separation of Pb(II) and Cu(II) in multicomponent systems. Zotzmann *et al.* [19] investigated chitosan modified by cross-linking with glutaraldehyde and genipin, but observed relatively low percentage removal, indicating that cross-linking alone does not substantially improve adsorption performance. Another approach involved incorporating fillers such as fuller's earth and aluminum silicate to enhance adsorption properties. Despite increased adsorption, this method also exhibited low selectivity, limiting its effectiveness for separating specific metal ions in complex systems [20]. Further studies have demonstrated the potential for functionalizing the chitosan polymer chain to improve metal adsorption efficiency. However, these conventional organic synthesis methods require toxic chemicals and harsh conditions, including elevated temperatures [21, 22].

To address these challenges, this project adopted a solvent-free mechanochemical synthesis to improve process sustainability. Mechanochemistry is a branch of chemical synthesis that employs mechanical forces, including compression, shear, and friction to drive chemical reactions. The required energy is typically delivered via grinding or milling, which facilitates bond breaking and formation without conventional solvent-based reaction media. Its principal advantage is the elimination or substantial reduction of toxic solvents, which allows the production of new chemical compounds in accordance with the principles of green chemistry [15, 23].

The objective of this study was to develop a adsorbent capable of selectively separating lead(II) ions from copper(II) ions. To achieve this, the ligand compound 4-(2-pyridylazo)resorcinol (PAR), which exhibits a strong affinity for forming complexes with certain metal ions, such as lead [24–26], was modified and used to synthesise a chitosan complex via a mechanochemical method. The resulting modified chitosan was then evaluated for its ability to separate lead ions from co-occurring copper ions in the target solution.

2. Materials and Methods

2.1. Materials

Chloroform, analytical grade (Chempur); PAR 4-(2-pyridylazo)resorcinol 96% (Sigma Aldrich); chitosan powder with a molecular weight of 100–300 kDa (Thermo Fisher Scientific), glacial acetic acid 99.5–99.9% (Poch S.A. Poland), epichlorohydrin 99.0% (Sigma Aldrich); glutaraldehyde 25% aqueous solution containing methanol (Sigma Aldrich); lead(II) nitrate p.a. (Poch S.A. Poland); copper(II) nitrate p.a. (Poch S.A. Poland); sodium hydroxide 99.4% p.a.; (Pureland, Poland), nitric acid 65% for analysis (Supelco, USA), hydrochloric acid 35–38% (Poch S.A. Poland); standard copper solution 1000 mg/dm^3 in HNO_3 (Merck, Germany); standard lead solution 1000 mg/dm^3 in HNO_3 (Merck, Germany) were used throughout this study. The water used was purified by a Millipore Elix 10 system (Merck Millipore).

2.2. Laboratory Equipment

Analytical balance (Radwag, As 220/X), technical balance (Radwag, Wtc 200), magnetic stirrer (Chemland, Ms-H-Pro), shaker (Chemland, Sk-O330-Pro), water bath (Chemland, Dk-2000-Iiil), Inductively Coupled Plasma Optical Emission Spectrometer (ICP-OES) (Varian 720-Es), Nuclear Magnetic Resonance (NMR) spectrometer (Agilent Magnet

400 MHz), Fourier transform infrared (FTIR) spectrometer (Nicolet 6700, Thermo Fisher Scientific), conductometer (ELMETRON) were applied during the various procedures.

2.3. Analytical Methods

Structural analysis of the synthesised ligand and the resulting chitosan derivative was performed using the Attenuated Total Reflection method on an FT-IR spectrometer. ^{13}C NMR analysis was performed by dissolving the sample in d6-DMSO. Elemental analysis of the solutions in the adsorption experiment was performed using an ICP-OES spectrometer. The following spectral lines were selected for the analysis of metal content in the samples: Cu: λ = 213.598, 224.700, 324.754, and 327.395 nm; Pb: λ = 182.143, 217.000, 220.353, 261.417, and 283.305 nm.

2.4. Sorbents Preparation Methods

2.4.1. Ligand Synthesis

0.500 g of PAR was weighed on an analytical balance and transferred to a flask. Then, 8 mL of chloroform, 4 mL of 50% aqueous sodium hydroxide solution, and finally 6 mL of deionised water were added. The reaction flask was equipped with a magnetic stirrer and a reflux condenser. The reaction was carried out at 328 K with intensive stirring (250 rpm) for 24 h. The post-reaction mixture was cooled to room temperature and acidified with a 1 M hydrochloric acid solution to pH 3.5. The acidified solution was transferred to a separator and extracted with two portions of chloroform, each 30 mL [27, 28]. The extract was evaporated to obtain an orange-red substance, which was stored in a glass container until use. The substance obtained is designated as PAR' in the following section of this article. The reaction scheme is given in Figure 1.

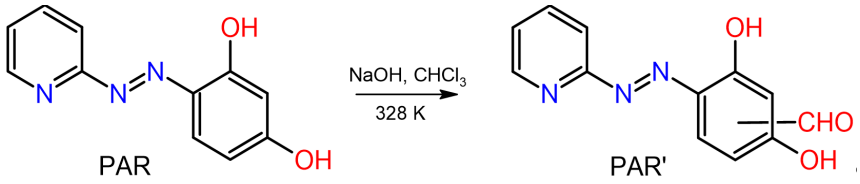

Figure 1. The reaction scheme of ligand derivative (PAR') synthesis.

2.4.2. Chitosan Modification

0.160 g of chitosan and 0.016 g of PAR' were placed in an agate mortar (10:1 mass ratio, PAR'-10). The reagents were intensively ground for 30 min and yielded a homogeneous orange powder [29]. The procedure was repeated for a different reagent mass ratio, i.e. by using 0.140 g of chitosan and 0.035 g of PAR' (4:1 mass ratio, PAR'-4), resulting in two different products.

2.4.3. Hydrogel Preparation

0.200 g of chitosan was weighed to prepare its 2% solution in 1% acetic acid. The obtained mixture was dripped through a needle into a 10% aqueous NaOH. The resulting hydrogels were left in the coagulating solution for 24 h, then filtered and washed with deionised water until the post-processed effluents reached a neutral pH and low conductivity (< 10 μS/cm). A similar procedure was performed by adding the substances as-prepared in Section 2.4.2. The hydrogels formed were denoted as CS, PAR'-4, and PAR'-10.

The obtained hydrogels were divided into two parts with similar, known masses. One of them was transferred into a 5% glutaraldehyde (GLU) solution, and the other into

an alkaline 0.5 M aqueous epichlorohydrin (EPI) solution. The hydrogels were cross-linked for 3 h at room temperature (for GLU) and at 318 K (for EPI) [30], then separated from the cross-linking agents, washed with deionised water and placed in a fresh portion of this water. The following adsorbents were obtained: CS-GLU, PAR'-4-GLU, PAR'-10-GLU, CS-EPI, PAR'-4-EPI, and PAR'-10-EPI.

2.5. Batch Adsorption Studies

Adsorbents and a model solution at pH 6 containing copper and lead at 10 mg/dm^3, with a solution-to-sorbent mass ratio of 50:1, were introduced into 25 mL flasks. Each flask was sealed with ground glass stoppers and shaken at room temperature for 24 h at 180 rpm. Then, the adsorbents were separated by analytical filters, and the resulting solutions were analysed by ICP-OES. Each test was performed twice.

2.6. Calculations and Statistical Analysis

Based on the results obtained from the ICP-OES analysis, the adsorption process of the adsorbents was characterised using two parameters: removal rate (R [%]) and lead ions selectivity coefficient (S_{Pb}):

$$R = \frac{(C_0 - C_e)}{C_0} \cdot 100\% \quad (1)$$

$$S_{Pb} = \frac{K_{Pb}}{K_{Cu}} \quad (2)$$

where:

C_0 – concentrations of a given metal before adsorption [g/dm^3];
C_e – concentrations of a given metal after adsorption [g/dm^3];
K_{Pb} – equilibrium partition constant for lead ion;
K_{Cu} – equilibrium partition constant for copper ion.

The error bars shown in the graphs represent the standard uncertainty, calculated according to the following formula:

$$u_p = \frac{RSD}{\sqrt{n}} \quad (3)$$

where:

RSD – relative standard deviation;
n – number of measurements.

3. Results and Discussion

3.1. Effect of Adsorbent on Metal Ion Removal Efficiency

Six different adsorbents were obtained, varying in the cross-linking agent and PAR' ligand content (see section 2.4) and used in batch-adsorption studies. The results of these experiments are presented in Figures 2 and 3.

Figure 2 presents the removal efficiency of lead and copper ions using glutaraldehyde-cross-linked hydrogels. The adsorbent cross-linked with GLU, without the addition of the PAR' ligand (CS-GLU), showed a high degree of lead ion removal of 94.1%. At the same time, the degree of copper ion removal was relatively low (44.4%). The results show that the introduction of the PAR' ligand into that type of chitosan adsorbent causes a reduction in lead removal compared to the adsorbent without the addition of the ligand. This may be due to additional cross-linking of the PAR' ligand within the chitosan structure.

The modified PAR can contain multiple aldehyde groups (Figure 1) that form additional cross-links with chitosan, leading to a more compact matrix structure and reduced porosity. Due to the larger ionic radius of lead ions, compared with that of copper ions, lead diffusion and migration toward active adsorption sites are limited. Consequently, the removal of lead ions decreases.

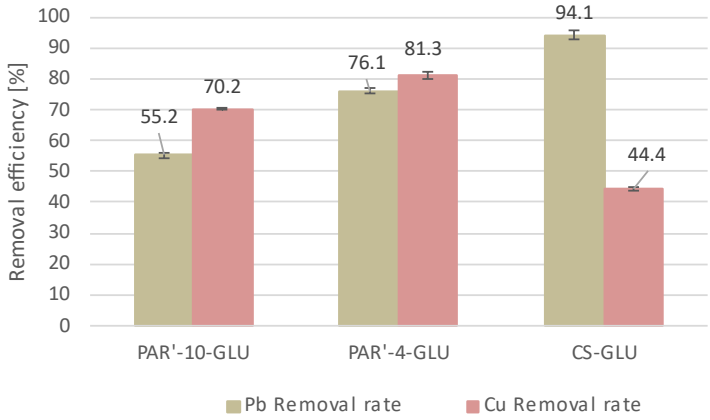

Figure 2. Influence of PAR' ligand in glutaraldehyde cross-linked adsorbents on the metal ion removal efficiency.

Figure 3 shows the results obtained for epichlorohydrin-cross-linked adsorbents. Because of the modification, the PAR'-4-EPI (of 1:4 ligand-to-chitosan mass ratio) and PAR'-10-EPI (of 1:10 ligand-to-chitosan mass ratio) adsorbents exhibited an increased removal efficiency for lead ions and a significantly decreased copper ions removal efficiency relative to the unmodified CS-EPI adsorbent. The results indicate that introducing the PAR' ligand into the chitosan structure improved the adsorption selectivity of epichlorohydrin-cross-linked adsorbents toward lead ions, but worsened it for copper ions. Compared with glutaraldehyde cross-linking, epichlorohydrin promotes the formation of dimers and oligomers, resulting in a more open adsorbent structure. This facilitates easier access of lead ions to the adsorbent matrix, which explains the higher efficiency of these materials for metal ions.

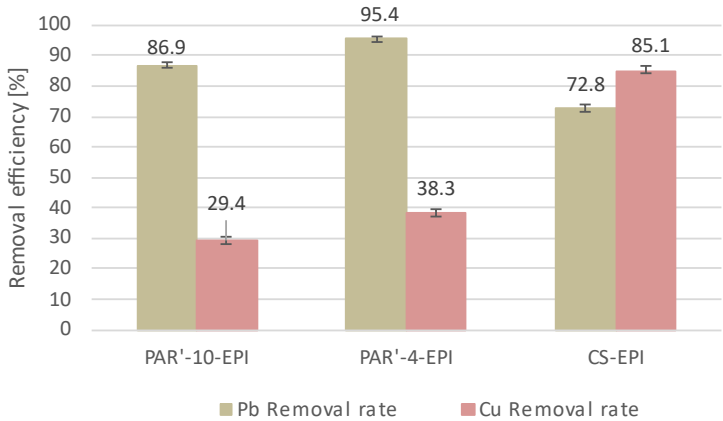

Figure 3. Influence of PAR' ligand in epichlorohydrin cross-linked adsorbents on the metal ion removal efficiency.

A comparison of the lead and copper removal efficiencies using adsorbents with different ligand contents revealed a consistent trend: the adsorbent with a higher ligand content (PAR'-4-EPI) demonstrated significantly greater removal efficiency than that with lower ligand loading (PAR'-10-EPI). This enhanced lead performance is likely due to the higher density of functional groups, which facilitates the transport of ions into the adsorbent matrix and explains the elevated metal uptake observed. Due to the strong affinity of copper ions for chitosan's primary amino groups, their partial immobilisation during functionalization with the PAR' ligand caused a notable drop in copper removal efficiency. Nevertheless, a subsequent increase in PAR' loading yielded a minor improvement in copper uptake. This behaviour suggests that copper ions also interact with the PAR' ligand, indicating that PAR' is not entirely selective toward lead and may exhibit a secondary affinity for other transition-metal ions, such as copper.

3.2. Effect of Adsorbent on Adsorption Selectivity

The selectivity of the synthesised adsorbents towards lead ions was assessed using the selectivity coefficient, calculated as described in section 2.6. Adsorbents with values of the coefficient lower than one were characterised by a greater affinity for the adsorption of copper ions. On the other hand, adsorbents with values greater than one showed higher selectivity towards lead ions.

Figure 4 summarises the selectivity coefficients of the tested adsorbents towards lead ions (S_{Pb}). Analysis of data on the relationship between the hydrogel cross-linking agent and its selectivity for lead ions shows that the adsorbent without ligand addition, cross-linked with glutaraldehyde (CS-GLU), exhibited greater selectivity than the adsorbent cross-linked with epichlorohydrin (CS-EPI). This result was likely driven by the distinct cross-linking mechanisms of glutaraldehyde and epichlorohydrin with chitosan. Glutaraldehyde binds to chitosan via nucleophilic attack on primary amino groups, forming Schiff bases and interconnected structures between polymer chains [31]. In contrast, epichlorohydrin cross-links chitosan by reacting with hydroxyl groups in an alkaline medium. This pathway leaves the highly complex primary amino groups unblocked [32]. Although the binding of both target metal ions occurs primarily through these remaining amino groups of chitosan, hydroxyl groups appear to play a critical role in the specific mechanism of lead ion adsorption. Consequently, the limited availability of hydroxyl groups in the epichlorohydrin-cross-linked matrix likely reduces the chitosan's adsorption selectivity for lead ions.

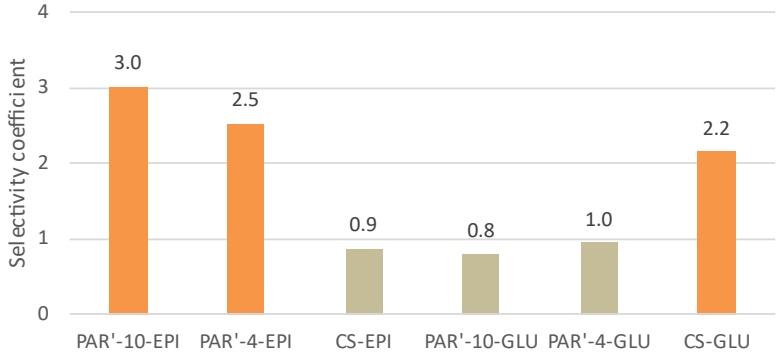

Figure 4. Selectivity of adsorbents depending on the cross-linking agent and the amount of ligand introduced (red bars represent the adsorbents with favourable selectivity towards lead).

The introduction of the PAR' ligand into the chitosan structure significantly changed the selectivity of the adsorbents. For the epichlorohydrin-crosslinked adsorbents PAR'-4-EPI and PAR'-10-EPI, an increase in the lead selectivity coefficient is visible in comparison to the unmodified CS-EPI adsorbent, while for PAR'-4-GLU and PAR'-10-GLU adsorbents cross-linked with glutaraldehyde, a significant decrease in lead selectivity is noticeable in comparison to the unmodified CS-GLU adsorbent. The increase in the selectivity of lead ion adsorption on adsorbents with the introduced PAR' ligand and cross-linked with epichlorohydrin is associated with better access to active sites for lead ions and may indicate either a different mechanism of metal ion adsorption or a different method of cross-linking modified chitosan. The best selectivity was obtained for the PAR'-10-EPI adsorbent, with a selectivity coefficient of 3.0, and a slightly lower 2.5 for the PAR'-4-EPI adsorbent. Additional research is needed to fully understand the higher selectivity of the adsorbent in which a smaller amount of PAR' ligand (1/10 of the chitosan mass) was used during the synthesis, compared to the selectivity of that with a higher PAR' mass fraction. However, we assume that the higher selectivity toward lead ions observed for the adsorbent containing a lower amount of PAR' ligand may be related to the limited selectivity of PAR' toward Pb(II) ions. The likely reason for this relationship may be associated with the different complexation properties of Cu(II) and Pb(II) with PAR'. According to the literature, Cu(II) ions with PAR can form both 1:2 and 1:1 stoichiometric complexes, depending on the metal-to-ligand ratio. Consequently, a higher PAR' content may promote additional interactions with Cu(II), reducing the apparent selectivity toward Pb(II). In contrast, Pb(II) ions mainly form 1:1 complex with PAR', which may limit the contribution of additional PAR' groups [33].

Additionally, the observed differences in selectivity may also result from several factors, such as the degree and efficiency of cross-linking, the availability of amino and hydroxyl groups in the adsorbent structure, and the sizes of cavities and pores formed during cross-linking. Copper(II) and lead(II) ions have different ionic radii (73 pm and 119 pm, respectively, as calculated from Shannon's data assuming octahedral coordination) [34]. This means that the greater a given crosslinking agent's ability to form a branched structure, the more limited lead(II) ions' access to the sorption cavities may be.

The type of cross-linking agent plays a significant role in variations in metal accessibility to adsorption sites. The high selectivity of epichlorohydrin-cross-linked adsorbents with the addition of PAR' ligand for the removal of lead ions can be explained by the better availability of functional groups and the facilitated transport of these ions into the adsorbent. Epichlorohydrin may form ether bonds between chitosan chains via oligomeric structures, resulting in a more flexible and less dense network. Consequently, the increased distance between polymer chains and the larger free volume in the hydrogel may contribute to better diffusion and binding of larger Pb(II) ions. Therefore, although Cu(II) ions possess a higher charge density, which leads to better complexing properties than those of lead, the presence of many functional groups in the adsorbent structure and appropriately matched active-site sizes may favour the binding of lead ions.

3.3. Characterisation of PAR' and the Tested Adsorbent

3.3.1. FTIR Analysis of PAR and PAR' Ligands

The FTIR spectra of PAR and PAR' are shown in Figure 5. The vibration modes of plain PAR and PAR' are also detailed in Table 1. In the PAR spectrum (red plot), several characteristic absorption peaks confirm the presence of aromatic structures. The band at 3039 cm^{-1} corresponds to aromatic C-H stretching vibrations. Signals at 1614 and 1588 cm^{-1}, together with the doublet at 1474 and 1438 cm^{-1}, are attributed to C=C

stretching vibrations within the aromatic ring. Additionally, bands at 777, 741, and 653 cm^{-1} are assigned to out-of-plane C-H bending vibrations of the aromatic system. The absorption band associated with the azo group (-N=N-) is very weak and could be observed in the 1400–1500 cm^{-1} region, which, however, overlaps with the absorption range of the aromatic ring. The presence of hydroxyl groups in the structure is indicated by a broad band in the range of 2500–3400 cm^{-1}, assigned to O-H stretching vibrations, and by bands in the 1000–1260 cm^{-1} region corresponding to C-O stretching. The spectrum of this compound is consistent with spectra reported in the literature [35].

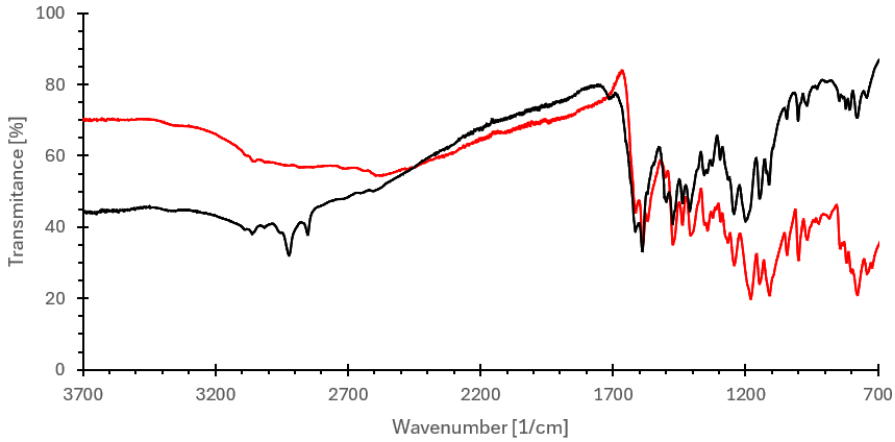

Figure 5. FTIR spectra of PAR (red plot) and its PAR' derivative (black plot).

Table 1. Vibration modes of plain PAR, PAR', CS, and CS-PAR'-4 samples.

Group and class	**Peak position [cm^{-1}]**			
	PAR	**PAR'**	**CS**	**CS-PAR'-4**
C–H stretching in the aromatic ring	3053	3059	-	3051
O–H, N–H combined stretching	3400–2500	3400–2500	3350, 3285	3350, 3283
C–H stretching of $–CH_2$ and –CH	-	-	2915, 2864	2919, 2849
C-H stretching in the -CHO group	-	2922, 2851	-	-
C=C stretching in the aromatic ring	1615, 1588	1615, 1589	-	1611, 1590
C=O stretching, amide I band	-	-	1665	-
N–H bending (overlapping with amide II)	-	-	1592	1592
C–H bending (including $–CH_2$ wagging)	-	1410	1373	1378
C–O and C–N stretching (including C–O–C bridge)	-	-	1150,1056, 1022	1151, 1066,
N–H and O–H out-of-plane bending modes	-	-	700–500	800–550

In the IR spectrum of the PAR' (Figure 5, black plot), the characteristic bands of the parent PAR framework are still visible. A band at 3061 cm^{-1} corresponds to aromatic C-H stretching, region 1614 and 1589 cm^{-1}, and another doublet at 1475 and 1437 cm^{-1} from C=C stretching; 777 and 742 cm^{-1} from aromatic C-H bending. The identification of the N=N bond remains challenging due to overlap with aromatic ring vibrations. The changes in the region 1600–1800 cm^{-1} (new absorption band and changes in band intensity and width), suggesting the appearance of C=O stretching vibrations, confirm the introduction of a carbonyl group into the structure. Further evidence for the aldehyde functionality is provided by the bands at 2922 and 2851 cm^{-1}, which correspond to C-H stretching vibrations of the -CHO group. These bands arise from Fermi resonance between the C-H stretching vibration and the overtone of the C-H deformation vibrations, which is characteristic of the aldehyde group [36, 37].

3.3.2. FTIR Analysis of CS and CS-PAR' Adsorbents

The vibration modes of plain CS and CS-PAR' are detailed in Table 1. In Figure 6, the unmodified CS and CS-PAR'-4 (sorbent prepared with a chitosan-to-ligand 4:1 mass ratio) spectra showed a broad combined signal with maxima at 3285 cm^{-1} and 3284 cm^{-1}, respectively. This suggests the stretching vibration of hydrogen connected with heteroatoms, i.e., from several chitosan –OH groups, deacetylated free $–NH_2$ groups, and –NH groups from acetylated units, and –OH groups from PAR' ligand [35]. At 2864 and 2919 cm^{-1}, the characteristic C-H stretching peaks from different $–CH_2$ and –CH groups in the chitosan structure were identified. The visible shifts toward high wavenumber between CS and CS-PAR'-4 suggest the incorporation of PAR' ligand in the structure of chitosan. A characteristic weak peak of the amide I band at 1665 cm^{-1} confirmed the existence of non-deacetylated amine groups in CS. In CS-PAR'-4 sample, this signal is not visible, which suggests that PAR' ligand reacted with this free amine group.

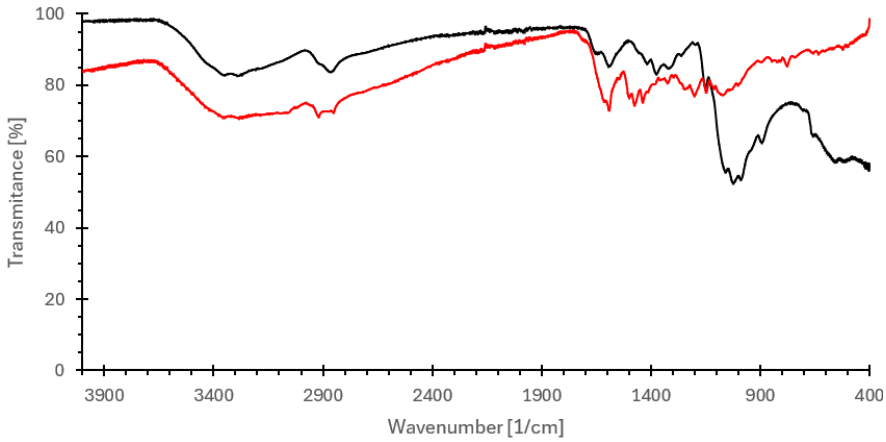

Figure 6. FTIR spectra of CS (black plot) and CS-PAR'-4 (red plot).

Moreover, the CS spectrum showed some bands specific for complex C-H deformation at 1415, 1370, 1314, and 1259 cm^{-1} coordinates, ether group (C-O-C stretching) at 1152 cm^{-1}, complex overlapped signal in 800–1100 cm^{-1} range with characteristic maxima corresponding to 1056, 1022, and 892 cm^{-1}, derived from secondary and primary hydroxyl groups (C-OH stretching) and primary amine groups (C-NH_2 stretching) [38].

For CS-PAR'-4 spectrum, in addition to the previously discussed bands, regions characteristic of both the PAR' ligand and chitosan can be observed. After the reaction with chitosan, the narrow bands at 2919 and 2849 cm^{-1} are weaker, which confirms that the formyl groups (CH=O) of the ligand have reacted with the amino groups of chitosan, which should result in the formation of an imine bond (N=C). Analysis of this type of bond in such a system is complicated by the presence of numerous absorbing bands in similar regions (the aromatic and pyridine rings, as well as the carbonyl group). Useful clues in the analysis of this system may be the changes in the area of 1600–1750 cm^{-1} (changes in the intensity and width of bands), suggesting the appearance of C=N stretching vibrations and the simultaneous decreasing of the intensity of the 1592 cm^{-1} absorption band (the amino groups) in the CS-PAR'-4 spectrum (red) compared to the CS spectrum (black). All the vibration modes discussed above of plain PAR, PAR', CS, and CS-PAR'-4 samples are summarised in Table 1. This table provides an overview of the distinct vibration characteristics of each sample, highlighting differences in their structural responses [36, 37].

3.3.3. ^{13}C NMR Analysis of PAR and PAR' Ligands

Figure 7a shows the ^{13}C NMR spectrum of PAR (substrate). The peak at 165.4 ppm corresponds to the (a') atom in the pyridine ring, and the peak at 162.4 ppm corresponds to the (d) carbon in the resorcinol ring, which is bonded to a hydroxyl group. Another carbon atom bonded to a hydroxyl group (f) gave a signal at 159.9 ppm. A group of peaks, whose signal positions will not change significantly after modification, consists of the remaining atoms of the pyridine ring (b', c', d', e'). Their signals are as follows: 111.6, 138.8, 123.8, 149.1 ppm. The signals of the following carbon atoms should be affected upon modification (Figure 1): the atom linking the resorcinol ring to the azo group (a) at 132.7 ppm, and the remaining atoms of this ring (b, c, e) at 131.9, 111.6, and 103.4 ppm [35].

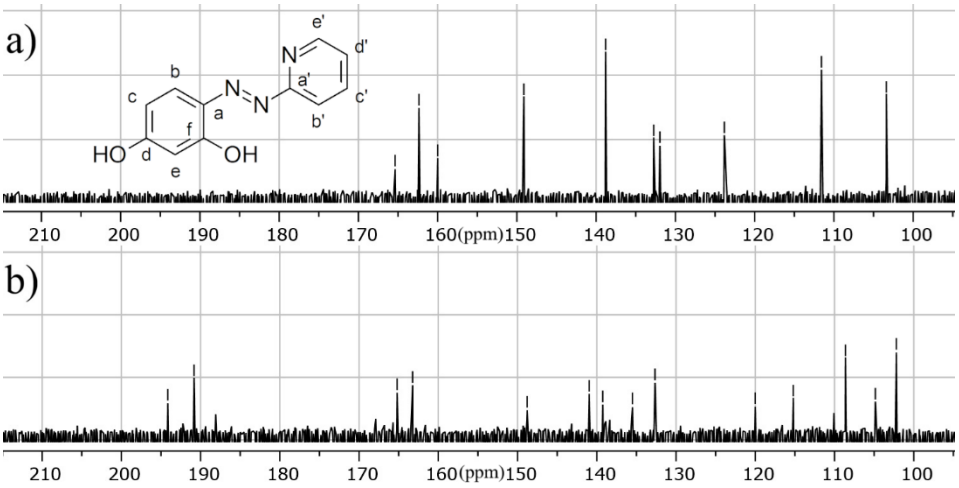

Figure 7. ^{13}C NMR spectra of (a) PAR and (b) PAR' samples (DMSO-d6/TMS).

The NMR spectrum of PAR' is significantly more complex, likely due to multiple isomers present in the sample (Figure 7b). The synthesis yields isomeric compounds that are difficult to separate due to their similar structures. Some signals from these isomers may overlap or diverge, resulting in up to 14 signals in the spectrum, even though each isomer

contains 12 distinct carbon atoms. The pyridine ring signals are similar to those in the PAR' (see the 165–149 ppm region). More changes are observed in the resorcinol ring signals; however, the most characteristic differences between the ^{13}C NMR spectra of PAR and PAR' appear at 194.1 ppm and 190.8 ppm (Figure 7b). These signals are characteristic of carbonyl compounds. They likely correspond to carbon atoms of the carbonyl groups, confirming the successful introduction of a formyl group (–CHO) into the compound. The most likely positions for the attachment of a formyl group (–CHO) are the (e) or (c) positions [36, 37].

3.4. Comparison of Lead and Copper Removal Methods

Table 2 highlights the high efficiency and outstanding selectivity of this system for Pb(II) during competitive co-adsorption in multicomponent matrices. The findings are compared with data from alternative methods and materials applied to similar separation systems, with essential experimental parameters provided alongside the capacity data to facilitate an objective comparison.

Table 2. Comparison of lead and copper removal efficiencies using various techniques.

Method		Removal [%]		S_{Pb}	Process parameters	[Ref]
		Pb	Cu			
precipitation		99.8	99.9	-*)	Na_2S – precipitation agent C_{Pb} = 100 mg/dm^3	[39]
electrocoagulation		98.8	89.9	-	t = 20–40 min J = 40–80 A/m^2 pH = 3–11 C_{Pb} = 10.92 mg/dm^3	[40]
liquid membrane extraction		92	-	1.47**)	C_{Pb} = 207.2 mg/dm^3 t = 30 min T = 293 K	[41]
Adsorption	activated carbon	97.5	76.4	-	single-component solution pH = 5–7 room temperature C_{Pb} = 20–50 mg/dm^3	[42]
	biochar	96	99	-	Cd also present pH = 1–5 T = 313–333 K C_{Pb} = 150–450 mg/dm^3	[43]
	chitosan	50	25	-	single-component solution pH = 6 C_{Pb} = 10 mg/dm^3	[44]
	resins	74.0	19.8	-	C_{Pb} = 50 mg/dm^3	[45]
	modified nanofiber	76	98.8	-	C_{Pb} = 250–2000 mg/dm^3	[46]
	PAR'-GLA	76.1	81.3	1	T = 278 K pH = 6 C_{Cu} = 10 mg/dm^3 C_{Pb} = 10 mg/dm^3	This study
	PAR'-EPI	95.4	38.3	2.5		This study

Note. *- no data available, ** - separation factor, S_{Pb} - lead ions selectivity coefficient.

Notably, while the newly developed materials demonstrate lead(II) uptake comparable to that of alternative adsorbents and existing separation methods, they exhibit a markedly lower affinity for copper(II) ions, as indicated by their substantially reduced uptake of Cu(II) relative to Pb(II) under identical conditions. Consequently, unlike previously documented methods, this system offers outstanding selectivity for Pb(II) during competitive co-adsorption in multicomponent matrices.

4. Conclusions

The development of advanced, efficient methods for water and wastewater treatment is essential to mitigate lead and copper contamination in the environment and reduce human exposure. As noted in the introduction, adsorption is a rapidly evolving technique that enables high-efficiency removal of pollutants, particularly at low concentrations commonly found in natural waters.

The synthesised adsorbents were characterised IR and NMR techniques, which confirmed both the formation of the derivative ligand PAR' and the successful mechanochemical reaction of PAR' with chitosan.

This study synthesised novel chitosan-based adsorbents, mechanochemically modified with the PAR' ligand, to enhance selectivity for lead ion adsorption from aqueous solutions containing both lead(II) and copper(II) ions. Adsorbents cross-linked with epichlorohydrin exhibited improved adsorption selectivity after the introduction of the PAR' ligand, whereas those cross-linked with glutaraldehyde showed greater selectivity without the ligand. Incorporating the PAR ligand into the adsorbent at a 1:10 mass ratio relative to chitosan increased the adsorbent's selectivity for lead ions in the presence of Cu(II) and led to high lead removal from solution.

It was found that this type of adsorbent has potential for separating binary mixtures containing copper(II) and lead(II) ions. Potential applications include sample concentration and metal ion determination in analytical chemistry, as well as water purification in sanitary engineering, thereby protecting human health and the environment. The proposed solution may also contribute to the development of comprehensive technologies for the separation of co-occurring lead and copper in water or industrial wastewater, such as from ammunition production by-products, in accordance with the concept of sustainable consumption and production.

Additionally, the developed chitosan-based materials closely match the adsorption performance of conventional adsorbents, including activated carbons, zeolites, and biochar. Crucially, their inherent biodegradability significantly enhances their environmental profile, positioning them as an optimal choice for green and sustainable applications.

5. Funding

The research was financed by the Rector of Silesian University of Technology as part of the 13th edition of the PBL project and the 6th and 7th editions of the project of the Chemistry Students Research Society of the Silesian University of Technology "Initiative of Excellence – Research University". The research was partially funded by the internal grants in the Silesian University of Technology: 04/010/BKM26/1132, 04/010/BK26/1120.

6. Author Contributions

Conceptualisation, P.K. and J.K.; methodology, T.M. and J.A.; formal analysis, P.K., Ł.W., and J.K.; investigation, P.K.; resources, J.A. and J.K.; data curation, P.K., Ł.W., J.A., and J.K.; writing—original draft preparation, P.K.; writing—review and editing, Ł.W. and J.K.; visualisation, P.K.; supervision, J.K.; project administration, Ł.W. and J.K.; funding acquisition, J.K. and Ł.W. All authors have read and agreed to the published version of the manuscript.

7. References

[1] Zaynab M, Al-Yahyai R, Ameen A, Sharif Y, Ali L, Fatima M, Khan KA, Li S; (2022) Health and environmental effects of heavy metals. Journal of King Saud University - Science 34(1), 101653. **DOI:** 10.1016/j.jksus.2021.101653

[2] Odobašić A, Šestan I, Begić S; (2019) Biosensors for determination of heavy metals in waters. In: Rinken T, Kivirand K (eds.), Biosensors for Environmental Monitoring, IntechOpen. **DOI:** 10.5772/intechopen.84139

[3] Wani AL, Ara A, Usmani JA; (2015) Lead toxicity: a review. Interdisciplinary Toxicology 8(2), 55–64. **DOI:** 10.1515/intox-2015-0009

[4] Badiye A, Kapoor N, Khajuria H; (2013) Copper toxicity: a comprehensive study. Research Journal of Recent Sciences 2, 58–67.

[5] Angelova M, Asenova S, Nedkova V, Koleva-Kolarova R; (2011) Copper in the human organism. Trakia Journal of Sciences 9(1), 88–89.

[6] Selinus O (ed.); (2005) Essentials of Medical Geology. Elsevier, Dordrecht.

[7] Levallois P, Barn P, Valcke M, Gauvin D, Kosatsky T; (2018) Public health consequences of lead in drinking water. Current Environmental Health Reports 5(2), 255–262. **DOI:** 10.1007/s40572-018-0193-0

[8] Samson CC, Masters SV, Mathews CL, Seidel CJ; (2024) Estimating the impact of the proposed Lead and Copper Rule Improvements. AWWA Water Science 6(5), e70004. **DOI:** 10.1002/aws2.70004

[9] EPA's Lead and Copper Rule Improvements; (2024). U.S. Environmental Protection Agency. Available online: https://www.epa.gov/system/files/documents/2024-10/lead-and-copper-rule-improvements-infographic_508.pdf (accessed: 26.03.2026).

[10] Arnold J; (2011) New insights into lead and copper corrosion: impacts of galvanic corrosion, flow pattern, potential reversal, and natural organic matter.

[11] Onyenanu CN, Onyenanu IU; (2025) Advanced treatment technologies for heavy metal removal from water and wastewater: a comprehensive review. International Journal of Applied and Natural Sciences 3(2), 111–131. **DOI:** 10.61424/ijans.v3i2.345

[12] Rashid R, Shafiq I, Akhter P, Iqbal MJ, Hussain M; (2021) A state-of-the-art review on wastewater treatment techniques: the effectiveness of adsorption method. Environmental Science and Pollution Research 28(8), 9050–9066. **DOI:** 10.1007/s11356-021-12395-x

[13] Fu F, Wang Q; (2011) Removal of heavy metal ions from wastewaters: A review. Journal of Environmental Management 92(3), 407–418. **DOI:** 10.1016/j.jenvman.2010.11.011

[14] Kaur S, Dhillon GS; (2014) The versatile biopolymer chitosan: potential sources, evaluation of extraction methods and applications. Critical Reviews in Microbiology 40(2), 155–175. **DOI:** 10.3109/1040841X.2013.770385

[15] Omer AM, Dey R, Eltaweil AS, Abd El-Monaem EM, Ziora ZM; (2022) Insights into recent advances of chitosan-based adsorbents for sustainable removal of heavy metals and anions. Arabian Journal of Chemistry 15(2), 103543. **DOI:** 10.1016/j.arabjc.2021.103543

[16] Lehocký M; (2025) Environmental applications of chitosan derivatives and chitosan composites. Polymers 17(19), 2583. **DOI:** 10.3390/polym17192583

[17] Negm NA, Hefni HHH, Abd-Elaal AAA, Badr EA, Abou Kana MTH; (2020) Advancement on modification of chitosan biopolymer and its potential applications. International Journal of Biological Macromolecules 152, 681–702. **DOI:** 10.1016/j.ijbiomac.2020.02.196

[18] Rangel-Mendez JR, Monroy-Zepeda R, Leyva-Ramos E, Diaz-Flores PE, Shirai K; (2009) Chitosan selectivity for removing cadmium (II), copper (II), and lead (II) from aqueous phase: pH and organic matter effect. Journal of Hazardous Materials 162(1), 503–511. **DOI:** 10.1016/j.jhazmat.2008.05.073

[19] Zotzmann J, Feldbusch E, Kruppke I, Aibibu D, Regenspurg S; (2023) Removal of lead and copper ions from geothermal brine at various temperatures and salinities using chemically crosslinked chitosan. Applied Geochemistry 155, 105733. **DOI:** 10.1016/j.apgeochem.2023.105733

[20] Kandil H, El-Wakeel ST; (2024) Effective removal of Pb(II) and Cu(II) from aqueous solutions using a hybrid composite of fuller's earth, aluminum silicate and chitosan. Polymer Bulletin 81(2), 1839–1859. **DOI:** 10.1007/s00289-023-04792-8

[21] Liu X, Zhao X, Liu Y, Zhang T; (2022) Review on preparation and adsorption properties of chitosan and chitosan composites. Polymer Bulletin 79(4), 2633–2665. **DOI:** 10.1007/s00289-021-03626-9

[22] Thambiliyagodage C, Jayanetti M, Mendis A, Ekanayake G, Liyanaarachchi H, Vigneswaran S; (2023) Recent advances in chitosan-based applications—a review. Materials 16(5), 2073. **DOI:** 10.3390/ma16052073

[23] Takacs L; (2013) The historical development of mechanochemistry. Chemical Society Reviews 42(18), 7649–7659. **DOI:** 10.1039/c2cs35442j

[24] Rodríguez-Maese R, Ferrer L, Cerdà V, Leal LO; (2020) Fully automatic system for lead monitoring in water. Microchemical Journal 154, 104550. **DOI:** 10.1016/j.microc.2019.104550

[25] Geary WJ, Nickless G, Polland FH; (1962) The metal complexes of some azo and azomethine dyestuffs. Analytica Chimica Acta 26, 575–582. **DOI:** 10.1016/S0003-2670(00)88433-0

[26] Geary WJ, Nickless G, Pollard FH; (1962) The metal complexes of some azo and azomethine dyestuffs. Analytica Chimica Acta 27, 71–79. **DOI:** 10.1016/S0003-2670(00)88452-4

[27] Tariq Z, Adnan S; (2019) Statistical evaluation of spectrophotometric determination of nickel(II) using Micelle-mediated extraction. Journal of Physics: Conference Series 1294(5), 052064. **DOI:** 10.1088/1742-6596/1294/5/052064

[28] Gusti Ngurah BIM, Jumina, Anwar C, Mustofa; (2014) Synthesis and characterization of octaethoxycalix[4]arene for heavy metal cations adsorbent. Advanced Materials Research 1043, 81–84. **DOI:** 10.4028/www.scientific.net/AMR.1043.81

[29] Van Poucke C, Mangelinckx S, Stevens CV; (2025) Shaking up conjugates between chitosan and aldehydes *via* mechanochemistry. RSC Mechanochemistry 2(1), 142–151. **DOI:** 10.1039/D4MR00110A

[30] Thakur A, Wanchoo RK, Soni SK; (2014) Chitosan hydrogel beads: a comparative study with glutaraldehyde, epichlorohydrin and genipin as crosslinkers. Journal of Polymer Materials 31(2), 211–223.
[31] Kildeeva NR, Perminov PA, Vladimirov LV, Novikov VV, Mikhailov SN; (2009) About mechanism of chitosan cross-linking with glutaraldehyde. Russian Journal of Bioorganic Chemistry 35(3), 360–369. **DOI:** 10.1134/S106816200903011X
[32] Miao L *et al.*; (2025) Epichlorohydrin cross-linked chitosan for adsorption of reactive red 2 dye: Optimization and adsorption mechanism. International Journal of Biological Macromolecules 320(4), 146202. **DOI:** 10.1016/j.ijbiomac. 2025.146202
[33] Kocyła A, Pomorski A, Krężel A; (2015) Molar absorption coefficients and stability constants of metal complexes of 4-(2-pyridylazo)resorcinol (PAR): Revisiting common chelating probe for the study of metalloproteins. Journal of Inorganic Biochemistry 152, 82–92. **DOI:** 10.1016/j.jinorgbio.2015.08.024
[34] Shannon RD; (1976) Revised effective ionic radii and systematic studies of interatomic distances in halides and chalcogenides. Acta Crystallographica Section A 32(5), 751–767. **DOI:** 10.1107/S0567739476001551
[35] SDBS; (1999). Available online: https://sdbs.db.aist.go.jp/CNmrSpectralView .aspx?imgdir=cds&fname=CDS10089&sdbsno=6891 (accessed: 19.03.2026).
[36] Zieliński W, Rajca A (eds.); (2018) Metody spektroskopowe i spektrometria mas w zastosowaniu do identyfikacji związków organicznych. Tom 1. Wydawnictwo Politechniki Śląskiej, Gliwice.
[37] Silverstein RM, Webster FX, Kiemle D; (2005) Spectrometric Identification of Organic Compounds, 7th Edition. Wiley.
[38] Czechowska-Biskup R, Jarosińska D, Rokita B, Ulański P, Rosiak J; (2012) Determination of degree of deacetylation of chitosan - comparision of methods. Progress on Chemistry and Application of Chitin and its Derivatives 2012, 5–20.
[39] Chen Q, Yao Y, Li X, Lu J, Zhou J, Huang Z; (2018) Comparison of heavy metal removals from aqueous solutions by chemical precipitation and characteristics of precipitates. Journal of Water Process Engineering 26, 289–300. **DOI:** 10.1016/ j.jwpe.2018.11.003
[40] Prasetyaningrum A, Ariyanti D, Widayat W, Jos B; (2021) Copper and lead ions removal by electrocoagulation: process performance and implications for energy consumption. International Journal of Renewable Energy Development 10(3), 415–424. **DOI:** 10.14710/ijred.2021.31665
[41] Mesli M, Belkhouche N-E; (2018) Extraction and pre-concentration of lead from copper by emulsion liquid membrane technique using an ionic liquid. Euro-Mediterranean Journal for Environmental Integration 3(1), 14. **DOI:** 10.1007/ s41207-018-0052-2
[42] Dowlatshahi S, Haratinezhad Torbati AR, Loloei M; (2014) Adsorption of copper, lead and cadmium from aqueous solutions by activated carbon prepared from saffron leaves. Environmental Health Engineering And Management Journal 1(1), 37–44.
[43] Ding E, Wang S, Zhao K, Li X, Zhao Z; (2026) Mechanistic insights into selective Pb(II) removal by magnetic sludge-derived biochar: A combined experimental and DFT study. Journal of Environmental Management 405, 129779. **DOI:** 10.1016/ j.jenvman.2026.129779
[44] Pham QM, Nguyen TH, Nguyen MK, Hoang MT, Pham HG, Vu A-T; (2026) Novel chitosan/g-C3N4 nanocomposite for Pb(II) removal: facile synthesis,

adsorption mechanism, and environmental applications. Environmental Science and Pollution Research 33(8), 3459–3480. **DOI:** 10.1007/s11356-026-37497-2

[45] Lee C-G, Jeon J-W, Hwang M-J, Ahn K-H, Park C, Choi J-W, Lee S-H; (2015) Lead and copper removal from aqueous solutions using carbon foam derived from phenol resin. Chemosphere 130, 59–65. **DOI:** 10.1016/j.chemosphere.2015.02.055

[46] Rajabi S, Shaki H; (2021) Efficient removal of lead and copper from aqueous solutions by using modified polyacrylonitrile nanofiber membranes. Fibers and Polymers 22(3), 694–702. **DOI:** 10.1007/s12221-021-0284-7

© Polish Chitin Society
Open Access: This article is distributed under the terms of the Creative Commons Attribution 4.0 International License (CC BY 4.0), which permits use, sharing, adaptation, distribution and reproduction in any medium or format, provided that appropriate credit is given to the original author(s) and source, a link to the license is provided, and any changes are indicated. Third-party material is included under the same license unless otherwise stated in a credit line.